Coarse-grained effective Hamiltonian via the Magnus Expansion for a three-level system

Nicola Macrì 1,2,* D, Luigi Giannelli 1,3 D, Elisabetta Paladino 1,2,3 D and Giuseppe Falci 1,2,3 D

- Dipartimento di Fisica e Astronomia "Ettore Majorana", Università di Catania, Catania, Italy
- INFN, Sezione di Catania 95123, Catania, Italy
- CNR-IMM, UoS Università 95123, Catania, Italy
- Correspondence: nicola.macri@dfa.unict.it

Abstract: Quantum state processing is one of the main tools of quantum technologies. While real systems are complicated and/or may be driven by non-ideal control they may nevertheless exhibit simple dynamics approximately confined to a low-energy Hilbert subspace. Adiabatic elimination is the simplest approximation scheme allowing us to derive in certain cases an effective Hamiltonian operating in a low-dimensional Hilbert subspace. However, these approximations may present ambiguities and difficulties hindering a systematic improvement of their accuracy in larger and larger systems. Here we use the Magnus expansion as a systematic tool to derive ambiguity-free effective Hamiltonians. We show that the validity of the approximations ultimately leverages only on a properly done coarse-graining in time of the exact dynamics. We validate the accuracy of the obtained effective Hamiltonians with suitably tailored fidelities of quantum operations.

Keywords: low-energy Hamiltonian, leakage, adiabatic elimination

1. Introduction

In the last decade, the research in quantum physics is experiencing a second quantum revolution [1,2]. Huge efforts have been and are being made in developing and engineering quantum hardware and control [3] allowing to perform novel quantum tasks in computation [4], communication [5,6] and sensing [7,8]. When dealing with real-life quantum hardware, one possibly has to take into account the presence of states which are not populated during the dynamics but still affect it via virtual processes. Their number is exponentially growing with the size of the system and may produce various phenomena from the renormalization of coupling constants to leakage from the relevant "computational" Hilbert subspace. These non-relevant sectors can be removed if an effective Hamiltonian \hat{H}_{eff} is determined which describes the same dynamics of the original \hat{H} for relevant cases and it is of course much simpler than the original one. This is specially important for quantum control where a simpler Hamiltonian [9] may allow for analytical solutions or for faster convergence of numerical intensive algorithms such those based on optimal control theory [3] or reinforcement learning [10,11].

Adiabatic elimination (AE) is perhaps the simplest and still successful method to determine \hat{H}_{eff} eliminating from the dynamics states that are mostly not populated. However, this approach presents ambiguities and limitations (see § 3.1) pointed out for instance in Refs. [12,13] where they have been tackled using various techniques such as Green's function formalism [12] and exploiting Markov approximation in a Lippman-Schwinger approach [13]. A canonical method for computing low-energy effective Hamiltonians relies on the Schrieffer-Wolff transformation technique [14,15], i.e. searching for a suitable unitary transformation that decouples approximately the relevant and the non-relevant subspaces.

Here we propose a derivation of an effective coarse-grained Hamiltonian which is naturally free from the ambiguities and limitations mentioned above. The method is based on the Magnus expansion (ME) which expresses the solution of a differential equation into an exponential



check for updates

Citation: Macri, N.; Giannelli, L.;

Paladino, E.; Falci, G.; Coarse-grained effective Hamiltonian via the Magnus Expansion for a three-level system.

Preprints 2022, 1, 0. https://doi.

with regard to jurisdictional claims in published maps and institutional affiliations



Copyright: © 2022 by the authors. Licensee MDPI, Basel, Switzerland. This article is an open access article distributed under the terms and conditions of the Creative Commons Attribution (CC BY) license (https:// creativecommons.org/licenses/by/ 4.0/).

form [16,17]. Applied to the time-evolution operator U in a suitable coarse-graining time τ , it yields an approximation whose logarithm gives an effective Hamiltonian. In general, the result depends on τ which must be chosen, if possible, in a proper way depending on the values of the system parameters and the significance of the relevant dynamics obtained a posteriori. As a benchmark, we apply the method to a three-level system in Lambda configuration. We discuss the systematic improvement of the approximation and compare it with other strategies. We check the validity of the results by using various figures of merit, the long-time fidelity of quantum evolution being the most informative one.

2. Methods

2.1. Effective Hamiltonian by the Magnus expansion

The Magnus expansion is a mathematical tool that allows one to express the solution of a differential equation in an exponential form. We apply that to the time-evolution operator $U(t,t_0)$ of a quantum system which solves the Schrödinger equation $\dot{U}(t,t_0)=-i\,H(t)\,U(t,t_0)$ for initial condition $U(t_0,t_0)=\mathbb{1}$. The Magnus expansion allows to write the logarithm of $U(t,t_0)$ as a series, or, likewise

$$U(t,t_0) = e^{-i\sum_i F_i(t,t_0)}$$

The two lowest-order terms of the expansion are given by

$$F_{1} = \int_{t0}^{t} ds H(s),$$

$$F_{2} = -\frac{i}{2} \int_{t0}^{t} \int_{t0}^{s_{1}} ds_{1} ds_{2} [H(s_{1}), H(s_{2})]$$
(1)

with $s_1 > s_2$. The term F_1 yields the so-called average Hamiltonian (which is used, for example, in Ref. [18] to implement a super-adiabatic protocol without the need of a new interaction), while F_2 provides already an excellent approximation in most cases. Higher-order terms involve time-ordered integrals of higher-order nested commutators [16,17,19] and are reported in appendix A.1.

Coarse-graining of the dynamics is operated by first splitting the evolution operator into time-slices ¹

$$U(t,t_0) = \prod_j U\left(t_j + \frac{\tau}{2}, t_j - \frac{\tau}{2}\right) =: \prod_j U_j.$$

Then we consider the ME in the j-th sub-interval and truncate the series at a given order n

$$\frac{i}{\tau} \ln U_j \approx \frac{1}{\tau} \sum_{i=1}^n F_i(t_j | \tau) =: H_{\text{eff}}(t_j | \tau)$$

obtaining an effective Hamiltonian (for a brief discussion about convergence see Appendix A.2). The structure of the ME suggests that accuracy is related to the smallness of the commutator [H(t), H(t')] at different times, and it may increase by choosing a small enough τ . If at the same time τ can be chosen large enough, the fast dynamics in the integrals defining F_i is averaged out. When successful, this procedure defines a coarse-grained Hamiltonian $H_{\rm eff}(t_j)$ whose explicit dependence on τ is negligible. With the same degree of accuracy, we finally obtain the approximate time-evolution operator as

An efficient way to exploit the Magnus expansion is to look at the evolution operator $U(t, t_0)$ in a time slice $\tau = (t - t_0)/N$.

$$U(t,t_0) \approx \prod_j e^{-iH_{\text{eff}}(t_j)\tau} \approx \exp\left\{-i\int_{t_0}^t ds \ H_{\text{eff}}(s)\right\} =: U_{\text{eff}}(t,t_0)$$

2.2. Validation of the effective Hamiltonian

Our main goal is to find a relatively simple $H_{\rm eff}$ describing accurately the dynamics in a suitable "relevant" subspace. The dynamics taking outside this subspace is not important, so $H_{\rm eff}$ needs not to be accurate there. Since we are interested to the dynamics it is natural to compare the exact population histories and coherences for the low-energy dynamics with those obtained with $H_{\rm eff}$.

More compact and effective quantifiers can be defined by adapting to our problem standard metrics for operators in the Hilbert space, as the operatorial spectral norm or trace norm [20–25]. We anticipate that the effective Hamiltonian we are going to derive has a block diagonal structure, $H_{\rm eff} = P_0 \, H_{\rm eff} \, P_0 + (\mathbb{1} - P_0) \, H_{\rm eff} \, (\mathbb{1} - P_0)$ where the projection operator P_0 defines the relevant subspace. Since $[H_{\rm eff}, P_0] = 0$ both the relevant subspace and its orthogonal complement are invariant under the effective dynamics. Then a suitable quantifier is defined as a fidelity

$$F = \min_{|\psi_0\rangle} \left\{ |\langle \psi_0 | \mathcal{U}^{\dagger} \mathcal{U}_{\text{eff}} | \psi_0 \rangle|^2 \right\}$$
 (2)

where $|\psi_0\rangle=P_0|\psi_0\rangle$ is a vector belonging to the relevant subspace. This subspace fidelity can be smaller than one either because $H_{\rm eff}$ is not accurate in describing the dynamics in the relevant subspace or because the exact dynamics determines leakage from the relevant subspace, with probability $L=\langle\psi_0|U^\dagger(t)\,[\mathbb{1}-P_0]\,U(t)|\psi_0\rangle$. Therefore we could define another figure of merit characterizing procedures where leakage from the subspace has been excluded by post-selection

$$F' = \min_{|\psi_0\rangle} \left\{ \left| \frac{\langle \psi_0 | \mathcal{U}^{\dagger} P_0}{\sqrt{1 - L}} \, \mathcal{U}_{\text{eff}} | \psi_0 \rangle \right|^2 \right\} = \min_{|\psi_0\rangle} \left\{ \frac{|\langle \psi_0 | \, \mathcal{U}^{\dagger} \mathcal{U}_{\text{eff}} | \psi_0 \rangle|^2}{1 - L} \right\} \tag{3}$$

which is the subspace fidelity between the effective dynamics and the post-selected vector. The impact of leakage will be quantified by approximating $F' \approx F_m' := F + L_m$ where L_m is the probability of leakage evaluated for the initial state which enters the minimization determining F in Eq.(2). This approximation is justified if both the infidelity and the leakage are small, $I := 1 - F \ll 1$ and $L \ll 1$, and arguing that while F_m' is not a lower bound as F' in Eq.(3) the worst-case error may be a significant overestimate for many initial states [20,21].

3. Application to adiabatic elimination

We now apply the procedure outlined to a three-level system in Lambda configuration modelled by the Hamiltonian

$$\hat{H} = -\frac{\delta}{2}|0\rangle\langle 0| + \frac{\delta}{2}|1\rangle\langle 1| + \Delta|2\rangle\langle 2| + \frac{1}{2}\sum_{k=0,1} \left[\Omega_k^* |k\rangle\langle 2| + \text{h.c.}\right]. \tag{4}$$

which describes a quantum network with on-site energies $(\pm\delta/2,\Delta/2)$ and tunneling amplitudes Ω_k (see Fig.1a). The same Hamiltonian provides the standard description in a rotating frame of a three-level atom driven by two near-resonant corotating semiclassical ac electromagnetic fields. In this case, Ω_k are the amplitudes of the fields while the single-photon detunings between the atomic level splitting E_i and the frequencies ω_k of the fields, $\delta_0 := E_2 - E_0 - \omega_0$ and $\delta_1 := E_2 - E_1 - \omega_1$, enter the diagonal elements $\delta := \delta_2 - \delta_1$ and $\Delta = (\delta_2 + \delta_1)/2$. This model describes several three-level coherent phenomena used in

quantum protocols from Raman oscillations [26,27], stimulated Raman adiabatic passage [28–30] and hybrid schemes [30,31].

The dynamics is governed by the Schrödinger equation $i\dot{c}_i(t) = \sum_{j=0}^2 \langle i|\hat{H}|j\rangle\,c_j(t)$ for i,j=0,1,2. The system is prepared in the subspace spanned by the two lowest energy states, i.e. $|\psi_0\rangle=c_0|0\rangle+c_1|1\rangle$, which is defined as the "relevant" subspace. We want to understand under which conditions the dynamics is confined to the relevant subspace, and to determine a Hamiltonian operator $\hat{H}_{\rm eff}$ whose projection onto this subspace effectively generates the confined dynamics.

3.1. Adiabatic elimination: ambiguities and limitations

AE offers a simple and handy solution to this problem [26]. The standard procedure [12, 13,26] relies on the observation that if $\Delta \gg \delta$, $|\Omega_k|$ for k=0,1, transitions from the lowest energy doublet and the state $|2\rangle$ are suppressed. Then, assuming then $\dot{c}_2(t)$ can be neglected in the Schrödinger equation, we find $c_2=-\frac{\Omega_0}{2\Delta}\,c_0-\frac{\Omega_1}{2\Delta}\,c_1$. Substituting in the equations for $\{c_0,c_1\}$ we obtain an effective two-level problem $i\partial_t|\phi\rangle=\hat{H}_{\rm eff}|\phi\rangle$ where

$$\hat{H}_{\rm eff} = -\left(\frac{\delta}{2} - S_0\right)|0\rangle\langle 0| + \left(\frac{\delta}{2} + S_1\right)|1\rangle\langle 1| + \left(\frac{\tilde{\Omega}}{2}|1\rangle\langle 0| + \text{h.c.}\right)$$

where $S_k = -|\Omega_k|^2/(4\Delta)$, k=0, 1 are energy shifts and $\tilde{\Omega} = -\Omega_0 \Omega_1^*/(2\Delta)$ is the normalized coupling. Since $\hat{H}_{\rm eff}$ is defined in the relevant subspace the state $|2\rangle$ is not involved in the problem anymore. This procedure may be generalized to d>3-level systems yielding an effective Hamiltonian in a n< d-dimensional relevant subspace.

It has been pointed out in the literature [12,13] that standard AE suffers from a number of ambiguities and limitations that here we summarize.

- 1. If we add to H a term $\eta \mathbb{1}$ which is an irrelevant uniform shift of all the energy levels, the procedure yields an $H_{\rm eff}$ which depends on η in a non-trivial way. Thus the procedure is affected by a gauge ambiguity. By comparing the exact numerical result with an analytic approximation based on the resolvent method a "best choice" $\eta=0$ has been proposed [12].
- 2. AE completely disregards the state $|2\rangle$. However, although apparently confining the dynamics to the relevant subspace the procedure yields that $c_2(t) \neq 0$ and depends on time. Thus, on the one hand the approximation misses leakage to $|2\rangle$; on the other, it does not guarantee that the normalization of states of the relevant subspace is conserved. In Ref. [13] the problem of normalization is overcome by writing separated differential equations in the relevant and in the non-relevant subspaces.
- 3. The residual population in $|2\rangle$ as given by the approximate $|c_2(t)|^2$ may undergo very fast oscillations with angular frequency $\sim \Delta$. This is not consistent with the initial assumption that $\dot{c}_2 \approx 0$. In Ref. [13] the assumption is supported by arguing that it holds at the coarse-grained level which averages out the dynamics at time-scales $\sim \Delta^{-1}$ or faster.
- 4. Standard AE is not a reliable approximation for larger two-photon detunings or larger external pulses and it is not clear how to systematically improve its validity.

We will show how the methodology outlined in § 2.1 yields an effective formulation which overcomes the whole criticism above leveraging only on coarse-graining of the dynamics.

3.2. Magnus expansion in the regime of large detunings

We now turn to coarse-graining via the ME. Having in mind the regime where $\Delta \gg |\Omega_k|$ we first transform the Hamiltonian Eq.(4) to the interaction picture

$$\tilde{H}(t) = U_0^{\dagger} (H - H_0) U_0 = \frac{\Omega_0^*}{2} |0\rangle\langle 2| e^{-i(\Delta + \delta/2)t} + \frac{\Omega_1^*}{2} |1\rangle\langle 2| e^{-i(\Delta - \delta/2)t} + \text{h.c.}$$

where $U_0(t) := e^{-iH_0t}$, H_0 being the diagonal part of H. The first two terms of the ME in Eqs.(1) are evaluated using the integrals reported in the Appendix B

$$\begin{split} \tilde{H}_{\mathrm{eff}}^{(1)}(t) &= \frac{\Omega_0^*}{2} \, e^{-i(\Delta+\delta/2)t} \, \mathrm{sinc}\Big(\frac{(\Delta+\delta/2)\tau}{2}\Big) \, |0\rangle\!\langle 2| + \\ &\quad + \frac{\Omega_1^*}{2} \, e^{-i(\Delta-\delta/2)t} \, \mathrm{sinc}\Big(\frac{(\Delta-\delta/2)\tau}{2}\Big) \, |1\rangle\!\langle 2| + \mathrm{h.c.} \\ \tilde{H}_{\mathrm{eff}}^{(2)}(t) &= S_0 |0\rangle\!\langle 0| + S_1 |1\rangle\!\langle 1| - (S_0 + S_1) |2\rangle\!\langle 2| + \frac{\tilde{\Omega}}{2} \, |1\rangle\!\langle 0| e^{i\delta t} + \mathrm{h.c.} \end{split}$$

where the coefficients are given by

$$S_k = -\frac{|\Omega_k|^2}{4(\Delta + (-1)^k \delta/2)} \left[1 - \operatorname{sinc}\left(\frac{\Delta + (-1)^k \delta/2}{2}\tau\right) \right],\tag{5}$$

$$\tilde{\Omega} = -\frac{\Omega_0 \Omega_1^*}{2} \frac{\Delta}{(\Delta^2 - \delta^4/4)} \left[\operatorname{sinc} \frac{\delta \tau}{2} - \operatorname{sinc} \frac{\Delta \tau}{2} \right], \tag{6}$$

for k=0,1. The first-order $\tilde{H}_{\rm eff}^{(1)}$ is an averaged version of \tilde{H} . The second-order $\tilde{H}_{\rm eff}^{(2)}$ contains shifts of the diagonal entries and an off-diagonal term coupling directly $|0\rangle$ and $|1\rangle$. At this order that state $|2\rangle$ is energy-shifted but not coupled to other states.

We now focus on the regime $\Delta \gg \delta$, $|\Omega_k|$ where we can choose a coarse-graining time such that $2\pi/\Delta \ll \tau \ll 2\pi/\delta$. Then all the $\mathrm{sinc}(x)$ functions appearing in the terms of H_{eff} above are nearly vanishing except for $\mathrm{sinc}(\delta\tau/2)\approx 1$. As a result first-order $\tilde{H}_{\mathrm{eff}}^{(1)}(t)$ averages out while the coefficients of $\tilde{H}_{\mathrm{eff}}^{(2)}(t)$ become

$$S_k = -\frac{|\Omega_k|^2}{4(\Delta + (-1)^k \delta/2)} \quad ; \quad \tilde{\Omega} = -\frac{\Omega_0 \Omega_1^*}{2} \frac{\Delta}{(\Delta^2 - \delta^4/4)}$$
 (7)

Transforming back to the laboratory frame we finally obtain

$$H_{\text{eff}} = -\left(\frac{\delta}{2} - S_0\right)|0\rangle\langle 0| + \left(\frac{\delta}{2} + S_1\right)|1\rangle\langle 1| + (\Delta - S_0 - S_1)|2\rangle\langle 2| + \frac{\tilde{\Omega}}{2}|1\rangle\langle 0| + \text{h.c.}$$

$$(8)$$

Before discussing the results in detail we make some general comments. As anticipated we obtain a a block-diagonal effective Hamiltonian. In the relevant subspace, it is similar to the result of standard AE. Concerning the criticism to the standard AE mentioned in § 3 we first observe that our result is not affected by the gauge ambiguity emerging for $H \to H + \eta \mathbb{1}$, the "best choice" rule $\eta = 0$ of Ref. [12] being set naturally. Indeed the uniform shift only changes trivially U_0 and does not enter \tilde{H} where only level splittings appear. Secondly, the state $|2\rangle$ is not eliminated but the block diagonal structure consistently preserves normalization in each subspace. Thus there is no need to assume that $\dot{c}_2 = 0$. Rather, Eq.(8) may describe also a three-level dynamics where all coherences oscillate. Finally, the ME obviously allows for

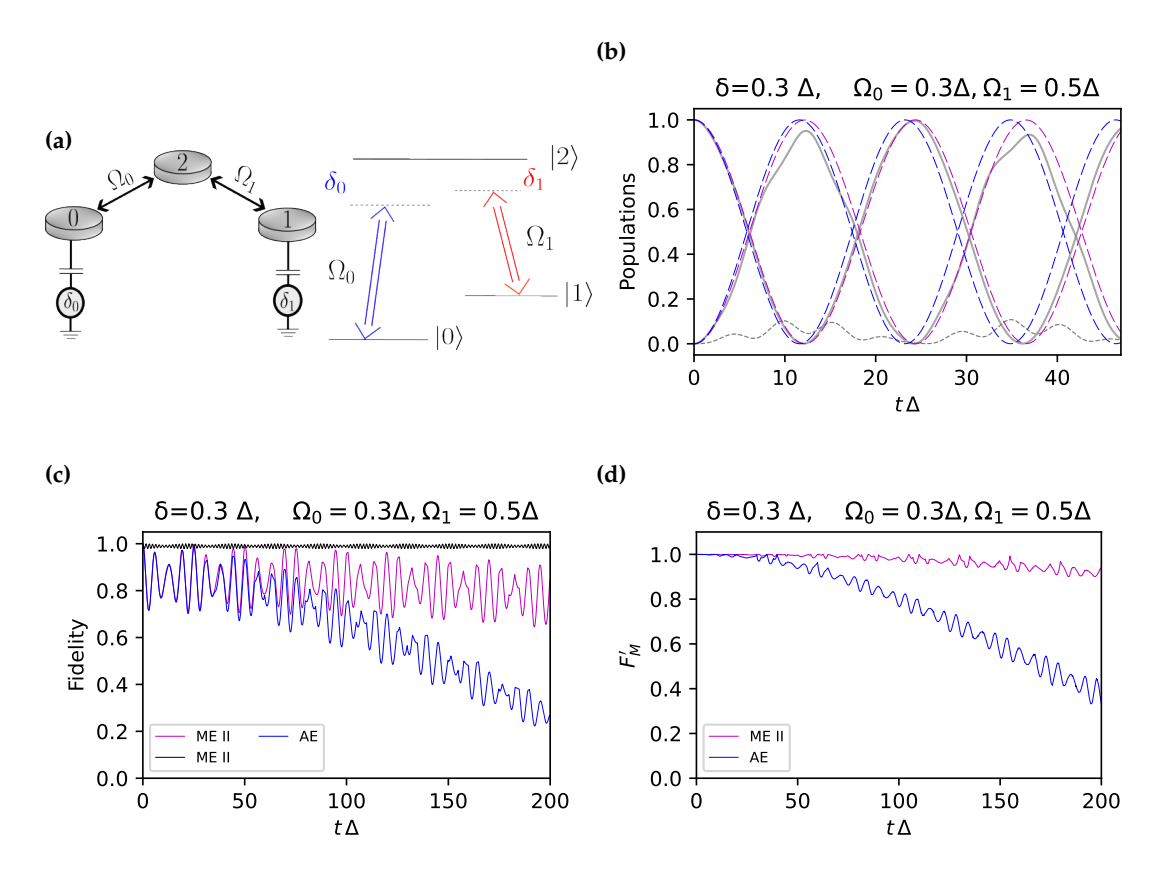


Figure 1. (a) The three-level model Eq.(4) describes for instance electronic levels confined in quantum dots Ω_k (on the left) representing tunneling amplitudes and δ_i gate voltages to the ground; alternatively it is the Hamiltonian in a rotating frame of a three-level atom (on the right) driven in Λ configuration, Ω_k and δ_i being amplitudes and detunings of the external fields. (b-d) Comparison between exact dynamics (grey curves) and effective dynamics obtained by ME (magenta) and standard AE (blue) for the parameters indicated in the figures. (b) population histories $|\langle \psi_0|U_i(t)|\psi_0\rangle|^2$, (curve starting from 1), $|\langle \psi_1|U_i(t)|\psi_0\rangle|^2$ (starting from 0) and $|\langle 2|U_i(t)|\psi_0\rangle|^2$ (gray dashed). (c) The two-level fidelity F Eq.(2) at larger times. The black line refers to values of (δ,Ω_k) four times smaller. (d) The fidelity for protocols with post-selection $F_m' = F + L_m$.

systematic improvement of the result of AE which moreover can be extended significantly as we will argue in the next sections.

While for $\delta=0$ our $H_{\rm eff}$ is identical to the "best choice" result of the standard AE differences emerge for $\delta\neq0$. Anticipating the quantitative analysis of § 3.2.1 here we point out that our $H_{\rm eff}$ reproduces correctly the shifts S_k as given by second-order perturbation theory² including the correct shift of the "eliminated" state $|2\rangle$. This feature is important for three-level of quantum operations and an example will be discussed later.

Coming back to coarse-graining there is still another time scale to take into account. The solution may describe Raman oscillations of the populations in the relevant subspace with a period $\sim 2\pi/|\tilde{\Omega}|$. Thus τ must be chosen small enough not to average out this dynamics while operating coarse-graining, which implies that $\Delta \gg \max(\delta, |\tilde{\Omega}|)$. In particular, for small δ we need $\Delta \gg |\tilde{\Omega}|$, implying that $|\Omega_0 \Omega_1|/(2\Delta^2) \ll 1$. Hence, in order the approximation to

If H describes a three-level atom under the action of corotating external fields S_k are the perturbative Stark shifts.

work, we don't need both amplitudes Ω_k to be small separately, provided their product is small. Notice finally that if δ increases, say $\delta\gg |\tilde{\Omega}|$, but we still may choose the coarse-graining time as $\tau\gg \max\left(2\pi/\Delta,2\pi/\delta\right)$, then Eq.(6) yields $\tilde{\Omega}\approx 0$. Differently from standard AE, the three-level $H_{\rm eff}$ resulting by ME correctly reduces in this limit to the diagonal energy-shifted form obtained by perturbation theory.

3.2.1. Comparison of the results at second-order

Besides overcoming the criticism raised to the standard AE, the ME approach gives a good approximation already at second order even when $|\Omega_0 \, \Omega_1|/(2 \, \Delta^2)$ is not very small. We here discuss the case $\delta \neq 0$ where results of the second-order ME differ from those obtained by standard AE. We first look at the population histories considering the dynamics from an initial state of the relevant subspace $|\psi_0\rangle = \cos\frac{\theta'}{2}|0\rangle + \sin\frac{\theta'}{2}|1\rangle$ with $\theta' = \theta + \frac{\pi}{2}$. For the curves in Fig. 1b the mixing angle θ' is chosen such that $|\psi_0\rangle$ is an eigenstate of an observable "orthogonal" in the Bloch space to the effective Hamiltonian obtained by standard AE. In other words, if this latter is represented by a vector forming an angle θ with σ_z then we take $\theta' = \theta + \pi/2$. This choice is expected to maximize the differences between the various cases.

Fig. 1b shows that coarse-graining by ME yields population histories that approximate better the exact dynamics in the relevant subspace. Notice that the discrepancy between ME and standard AE is very significant since it indicates a systematic error in the energies which accumulate over time. This clearly emerges from the fidelities F defined in Eq.(2) and shown in Fig. 1c where the minimization has been performed numerically. Indeed, F become small for the standard AE while the discrepancies between the ME result and the exact dynamics have a much smaller impact than what appears from the population histories. Actually, infidelity for the ME result is almost entirely due to leakage from the relevant subspace. These latter errors seem not to accumulate in time (magenta curve) as confirmed by the corresponding curve in Fig. 1d which shows that leakage errors can be corrected by post-selection. The residual error in the phase of the ME curves is remarkably small despite the exceedingly large value of $\sqrt{|\Omega_0 \Omega_1|/(2\Delta^2)} \approx 0.27$ we used and it is correctable by extending the analysis to fourth order as we will show in the next section. Errors due to leakage in Fig. 1c almost disappear for values $\sqrt{|\Omega_0 \Omega_1|/(2\Delta^2)} \ll 0.1$ (black curve in Fig. 1c), even smaller values being routinely used for control of solid-state artificial atoms. It is anyhow remarkable the accuracy of the ME coarse-grained second-order $H_{
m eff}$ in describing the protocol supplemented by post-selection for values of δ and Ω_k much beyond the perturbative regime.

3.2.2. Higher-order effective Hamiltonian

We now exploit the systematic improvement of the approximation. For the sake of simplicity, we will consider $\delta=0$. In this case, the exact eigenvalues can be calculated analytically, the two splittings $\epsilon_{ij}:=\epsilon_i-\epsilon_j$ being $\epsilon_{10}=\frac{\Delta}{2}\left(\sqrt{1+4\,x}-1\right)$ and $\epsilon_{21}=\frac{\Delta}{2}\left(\sqrt{1+4\,x}+1\right)$ where $x:=\left(|\Omega_0|^2+|\Omega_1|^2\right)/(4\,\Delta^2)$. The second-order $H_{\rm eff}$ in Eq.(8) reproduces the lowest-order expansion, $\epsilon_{10}/\Delta\approx x$ and $\epsilon_{21}/\Delta\approx 1+x$ and we now evaluate higher-order terms. Due to the algebra of the operators (see Appendix A.3) the important property holds that terms of odd orders have the same structure as $\tilde{H}_{\rm eff}^{(1)}$ while at even orders they have the structure of $\tilde{H}_{\rm eff}^{(2)}$. In particular the third-order term in the laboratory frame reduces to

$$H_{\mathrm{eff}}^{(3)} = \alpha(\tau) x \left(|2\rangle\langle 0| \frac{\Omega_0}{2} + |2\rangle\langle 1| \frac{\Omega_1}{2} \right) + \mathrm{h.c.}$$

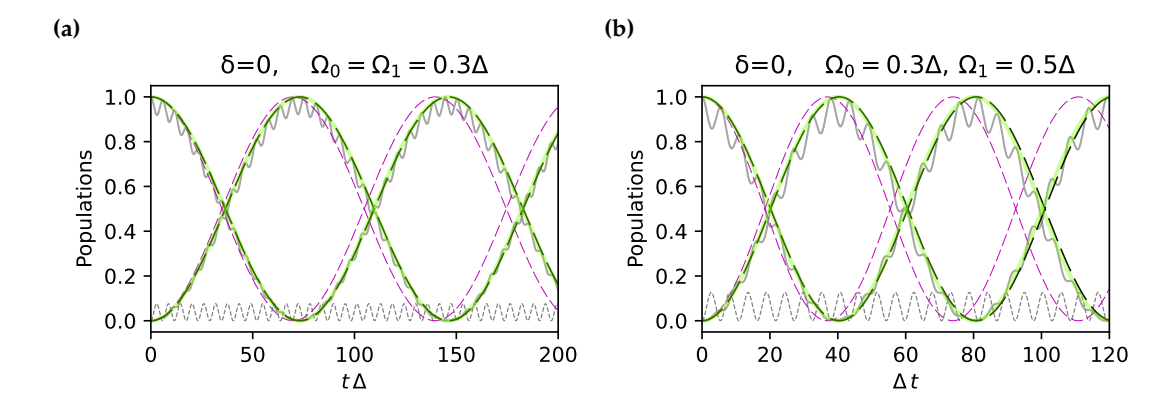


Figure 2. Population histories $|\langle \psi_0|U_i(t)|\psi_0\rangle|^2$, (curve starting from 1), $|\langle \psi_1|U_i(t)|\psi_0\rangle|^2$ (starting from 0) and $|\langle 2|U_i(t)|\psi_0\rangle|^2$ (gray dashed) for $\delta=0$. We compare for the exact dynamics (gray curves) and the higher-order approximate effective dynamics obtained by the second-order (magenta dashed) and fourth-order (black dashed) ME. This latter coincides with the first-order Markov approximation of Ref. [13] (light green curve).

where $\alpha(\tau) = 1 + \frac{1}{3}\operatorname{sinc}\frac{\Delta\tau}{2}\left[1 - 8\cos(\Delta\tau/2)\right]$ up to an irrelevant factor of modulus one depending on the detailed coarse-graining procedure.

After coarse-graining over a time $\tau\gg 2\,\pi/\Delta$ we are left with $\alpha(\tau)\approx 1$. The resulting term triggers transitions between the relevant and the not relevant subspaces. While $H_{\rm eff}^{(3)}$ is $\sim x^{3/2}$ being off-diagonal it contributes at order x^3 to the correction of the splittings as it can be shown by ordinary non-degenerate perturbation theory.

We turn to the fourth order of the ME whose full expression is reported in appendix B. After coarse-graining, the contribution to the effective Hamiltonian in the laboratory frame reduces to

$$H_{\text{eff}}^{(4)} = S_0^{(4)} |0\rangle\langle 0| + S_1^{(4)} |1\rangle\langle 1| + (\Delta - S_0^{(4)} - S_1^{(4)}) |2\rangle\langle 2| + \frac{1}{2} \left[\tilde{\Omega}^{(4)} |1\rangle\langle 0| + \text{h.c.} \right]$$
(9)

where $S_k^{(4)} = x |\Omega_k|^2/(4\Delta)$ and $\tilde{\Omega}^{(4)} = x \Omega_0 \Omega_1^*/(2\Delta)$. This term reproduces the expansion of the exact splitting up to order x^2 , providing a more relevant correction to $H_{\rm eff}^{(2)}$ Eq.(8) than the third-order $H_{\rm eff}^{(3)}$. Therefore we could neglect this latter term and approximate $H_{\rm eff} \approx H_{\rm eff}^{(2)} + H_{\rm eff}^{(4)}$. The above effective Hamiltonian reproduces both the exact energy splittings to order

The above effective Hamiltonian reproduces both the exact energy splittings to order x^2 . Being block-diagonal it admits no leakage. We may wonder if including $H_{\rm eff}^{(3)}$ may yield useful information on leakage, but the answer is negative. Indeed we checked that its impact on population histories is small. In particular, the ME yields a coarse-grained version of the population in $|2\rangle$ which is much smaller than the exact one since this latter oscillates on a time scale $\sim 2\pi/\Delta$.

3.2.3. Validation of the results at fourth-order

We now validate our result using the same quantifiers as in § 3.2.1. Population histories are shown in Fig. 2 for two different sets of parameters. It is seen that the fourth-order ME

³ Up to a phase factor depending on the modality of time slicing (see Appendix B).

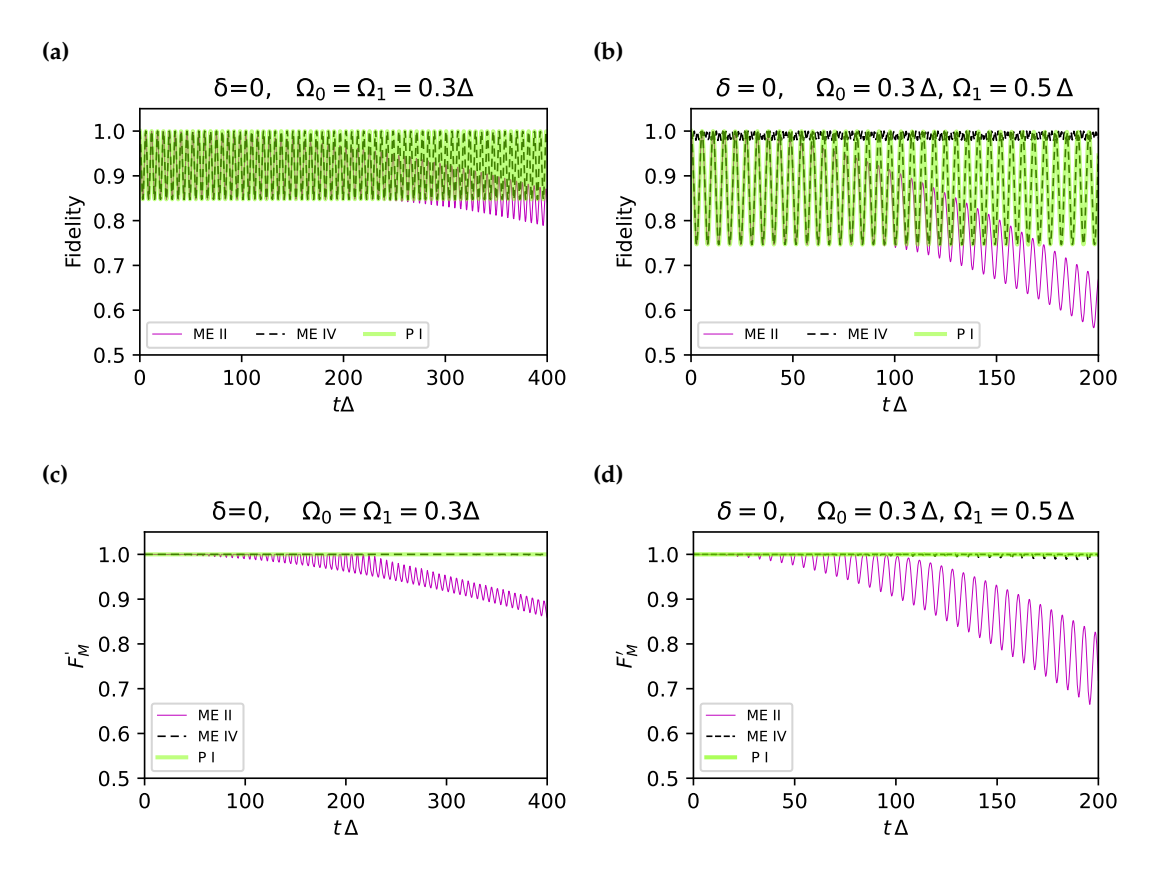


Figure 3. (a-b) Subspace fidelities F for the parameters indicated. The curves refer to the second-order ME (magenta) and to the fourth-order ME (black dashed), which practically coincides with the Lippmann-Schwinger approach in Markov approximation of Ref. [13] (green line). The second-order ME is affected by phase errors accumulating in time, whereas the error in the other two curves does not accumulate being due to leakage. In this latter case, F is still large considering the values of the parameters are well beyond the perturbative regime. The black solid line in panel (b) refers to values of (δ, Ω_k) four times smaller and also the leakage error disappears. (c-d) The fidelity for protocols with post-selection $F'_m = F + L_m$. The fourth-order ME (black dashed) and the approximation of Ref. [13] (green line) are remarkably accurate also for values of the parameters well beyond the perturbative regime.

(black dashed line) yields a coarse-grained version of the exact result (full gray line) which is accurate in reproducing the Raman oscillations between levels of the relevant subspace. On the contrary the second-order ME (dashed magenta line) clearly shows a discrepancy in the oscillation frequency. This error appears clearly in the long-time fidelity F, shown in Fig. 3(a-b), and the fidelity of post-selected protocols, shown in Fig. 3(c-d). In the same figures, we also compare the fourth-order ME with the approximation scheme proposed in Ref. [13] (green curves) and the two approaches are seen to coincide. Therefore the ME provides a systematic approximation scheme, overcoming the last point of the criticism to standard AE mentioned in § 3.1.

In particular for the symmetric choice $|\Omega_0| = |\Omega_1| = 0.3 \Delta$ (Figs. 3a, 3c) the fourth order fidelity oscillates between one and 0.8 (black dashed curve), whereas the second-order result (magenta dashed curve) decays to lower values because the error in frequencies accumulates in time. The same behaviour is obtained for the asymmetric configuration of the drive amplitudes shown in Figs. 3b, 3d. For these time scales the error in the fourth-order *F* in Figs. 3(a-b) does not

accumulate in time and Figs. 3(c-d) show that it is entireka:16-vepsalainen-photonics-squtritly due to leakage since it can be corrected by post-selection. Again we notice that in Figs. 2, 3 we used parameters with values far beyond the perturbative regime to magnify the errors. Still, errors are not so large and in particular, they are remarkably small for the post-selected dynamics. As in Fig. 1c, errors due to leakage in Fig. 3b (black curve) almost disappear already for values $\sqrt{|\Omega_0 \, \Omega_1|/(2 \, \Delta^2)} \ll 0.1$.

Finally, we stress the agreement of the ME result with the results of the approach of Ref. [13]. This latter achieves a high-level accuracy using an iterated Lippmann-Schwinger equation in a special gauge defining the interaction picture and supplementing the problem by an ad hoc assumption of Markovianity of the dynamics. Our approach based on the ME shows that the correct result only leverages on coarse-graining.

4. Discussion and conclusions

We introduced a technique based on the Magnus expansion that allows deriving a coarse-grained effective Hamiltonian and yielding a simplified model for the low-energy dynamics of the system. We applied the technique to the problem of the three-level lambda system clarifying ambiguities and inconsistencies of standard AE, which have been raised in the literature [12,13].

Results from ME accurately interpolate all the limiting cases obtained by standard approximations. For instance, the second-order ME yields a result reducing to the usual AE for $\delta \ll |\Omega_k|$ but reproducing the perturbative Stark shifts for $\delta \gg |\Omega_k|$. Moreover, the accuracy of the ME can be systematically increased reaching a full agreement with other accurate approximation schemes such as the one developed in Ref. [13]. Since the ME-based approximation we propose only relies on coarse-graining, this latter is identified as the key ingredient underlying all the approximations.

Coarse-grained based approximations yield effective Hamiltonians reproducing accurately the dynamics in the relevant subspace for a wide range of parameters, much beyond the perturbation regime. In particular, it is remarkably large the accuracy achieved for protocols supplemented by post-selection.

Notice that the ME approach we described yields a block diagonal effective Hamiltonian which does not cancel the not-relevant subspace but treats it consistently. In particular, for the Lambda system we obtain the correct perturbative energy shift for the level $|2\rangle$. This result allows non-trivial applications to problems involving multiphoton processes in three-level dynamics [27,32] which are relevant for newly developed quantum hardware [33–35].

Finally, the approach can be extended to the search for effective Hamiltonians in time-dependent problems. The extension is straightforward if the parameters of the Hamiltonian are slowly varying on time scales of the order of the coarse-graining time τ as in Ref. [36].

Author Contributions: Conceptualization and methodology: N.M., L.G., E.P. and G.F.; software: N.M.; validation: N.M., L.G., E.P. and G.F.; formal analysis: N.M., L.G., E.P. and G.F.; writing—original draft preparation, N.M.; writing—review and editing: L.G., E.P. and G.F.; visualization: N.M., L.G.; supervision: E.P. and G.F.; project administration, G.F.; funding acquisition: E.P. and G.F. All authors have read and agreed to the published version of the manuscript.

Funding: This work was supported by the QuantERA grant SiUCs (Grant No. 731473), by the University of Catania, Piano Incentivi Ricerca di Ateneo 2020-22, project Q-ICT, by the Partenariato Esteso "National Quantum Science and Technology Institute (NQSTI)" - ambito di intervento "4. Scienze e Tecnologie Quantistiche" and from ICSC – Centro Nazionale di Ricerca in High Performance Computing, Big Data and Quantum Computing, co-funded by European Union – NextGenerationEU.

Institutional Review Board Statement: Not applicable.

Data Availability Statement: Not applicable.

Acknowledgments: The authors acknowledge Giulia Termini for helpful discussions.

Conflicts of Interest: The authors declare no conflict of interest. The funders had no role in the design of the study; in the collection, analyses, or interpretation of data; in the writing of the manuscript; or in the decision to publish the results.

Abbreviations

The following abbreviations are used in this manuscript:

ME Magnus expansion AE Adiabatic elimination

Appendix A More on the ME

Appendix A.1 Third and fourth-order terms

We report here the higher-order terms we use in this work referring to [17] for more details. The third-order term is

$$F_3 = \frac{(-i)^2}{6} \int_{t_0}^t \int_{t_0}^{s_1} \int_{t_0}^{s_2} ds_1 ds_2 ds_3 \{ [H(s_1), [H(s_2), H(s_3)]] + [[H(s_1), H(s_2)], H(s_3)] \},$$

while at fourth order we have

$$F_{4} = \frac{(-i)^{3}}{12} \int_{t_{0}}^{t} \int_{t_{0}}^{s_{1}} \int_{t_{0}}^{s_{2}} \int_{t_{0}}^{s_{3}} ds_{1} ds_{2} ds_{3} ds_{4} \Big\{ [[[H(s_{1}), H(s_{2})], H(s_{3})], H(s_{4})] + \\ + [H(s_{1}), [[H(s_{2}), H(s_{3})], H(s_{4})]] + [H(s_{1}), [H(s_{2}), [H(s_{3}), H(s_{4})]]] + \\ + [H(s_{2}), [H(s_{3}), [H(s_{4}), H(s_{1})]] \Big\}.$$

Appendix A.2 Convergence

The convergence of the Magnus expansion depends on the necessary condition

$$\int_0^{\tau} \|\tilde{H}\| ds < \pi$$

where the spectral norm is intended [17,37]. This limit is a more version of $\tau \|\tilde{H}\| \ll 1$ [38] and it may be rather conservative. Indeed, the radius of convergence of the series may be larger [17]. For instance, for the Hamiltonian

$$\tilde{H}(t) = \frac{\Omega}{2} e^{-i\Delta t} \sum_{j < 2} |j\rangle\langle 2| + \text{h.c.}$$

the above sufficient convergence condition becomes $\tau < 2\pi/\Omega$ and it gives a rather conservative bound on the coarse-graining time τ .

Appendix A.3 Structure of the series for the Lambda Hamiltonian

The Lambda Hamiltonian we study has the structure

$$\tilde{H}(s) = \sum_{i=0,1} V_i(s)|i\rangle\langle 2| + \text{h.c.}$$

with $V_i(s) = \Omega_i e^{-i\epsilon_{2i}s}/2$. The second-order term of ME contains the commutator

$$C_{\mathrm{II}}(s,s') = \left[H(s), H(s')\right] = \sum_{i,j=0,1} f_{i,j}(s,s') \left(|2\rangle\langle 2|\,\delta_{i,j} - |j\rangle\langle i|\right) \tag{A1}$$

where $f_{i,j}(s,s') = V_i^*(s) V_j(s') - V_j(s) V_i^*(s')$ these terms come from $[|2\rangle\langle i|, |j\rangle\langle 2|]$. This structure yields shifts on the diagonal elements of the Hamiltonian and connects the states of the relevant subspace (see Eq. 8).

Going on with the third order, we encounter the nested commutator

$$C_{\text{III}}(s, s', s'') = [[H(s), H(s')], H(s'')] \sum_{i=0,1} g_i(s, s', s'') |i\rangle\langle 2| + \text{h.c.}$$
 (A2)

where $g_i(s,s',s'') = -\sum_{j=0,1} \left[f_{i,i}(s,s') \, V_j(s'') + f_{i,j}(s,s') \, V_i(s'') \right]$. This quantity has same structure of $\tilde{H}(s)$ and comes from $[|2\rangle\langle 2|, |i\rangle\langle 2|] = -|i\rangle\langle 2|$ and $[|i\rangle\langle j|, |k\rangle\langle 2|] = \delta_{j,k} \, |i\rangle\langle 2|$. This argument can be iterated showing that even (odd) nested commutators have the structure of Eq. A1 (Eq. A2).

Appendix B Integrals

In this work, the ME at order n requires the evaluation of time-ordered integrals of the form

$$\int_{t-\tau/2}^{t+\tau/2} dt_n \dots \int_{t-\tau/2}^{s_2} dt_1 e^{i\sum_{j=1}^n \omega_j t_j} = e^{i\sum_{j=1}^n \omega_j t} \int_{-\tau/2}^{\tau/2} ds_n \dots \int_{-\tau/2}^{s_2} ds_1 e^{i\sum_{j=1}^n \omega_j s_j}$$

If we shift the origin of the interval by $\tau/2$ the integral becomes

$$e^{i\sum_{j=1}^{n}\omega_{j}(t-\tau/2)}\int_{0}^{\tau}ds_{n}\dots\int_{0}^{s_{2}}ds_{1}e^{i\sum_{j=1}^{n}\omega_{j}s_{j}}.$$
 (A3)

The integral can be calculated at all orders and we find

$$\int_{0}^{\tau} ds_{n} \dots \int_{0}^{s_{2}} ds_{1} e^{i\sum_{j=1}^{n} \omega_{j} s_{j}} = (-i)^{n} \sum_{k=1}^{n} A_{k}^{n} \left(e^{i\Omega_{k-1}^{n} \tau} - 1 \right)$$

$$\Omega_{k-1}^{n} = \sum_{j=n-(k-1)}^{n} \omega_{j}, \qquad \Omega_{0}^{n} = \omega_{n}$$

$$A_{k}^{n} = \frac{A_{k-1}^{n-1}}{\Omega_{k-1}^{n}}, \qquad A_{0}^{n} = -\sum_{k=1}^{n} A_{n}^{k}, \qquad A_{1}^{1} = \frac{1}{\omega_{1}}$$
(A4)

We notice that the factor $e^{-i\sum_{j=1}^n \omega_j \tau/2}$ in the integral Eq.(A3) depends on the choice of time slicing for coarse-graining. Indeed if we choose to integrate between $[t,t+\tau]$ instead of $[t-\tau/2,t+\tau/2]$ this factor does not appear. We expect that this dependence is irrelevant in most cases. Indeed in our case this dependence appears only in the third-order term of the ME which we must consistently neglect at the order of accuracy of our calculations.

Using the integrals above we can calculate the fourt-order term of the ME which is given by

$$\tilde{H}_{\text{eff}}^{(4)} = \beta(\tau) \left\{ \frac{\tilde{\Omega}^{(4)}}{2} |0\rangle\langle 1| + \text{h.c.} + \sum_{k=0}^{1} S_k^{(4)} |k\rangle\langle k| - (\sum_{k=0}^{1} S_k^{(4)}) |2\rangle\langle 2| \right\}$$
$$\beta(\tau) = \left(1 - \frac{2}{3} \cos \frac{\Delta \tau}{2} \operatorname{sinc} \frac{\Delta \tau}{2} - \frac{1}{3} \cos \Delta \tau \operatorname{sinc} \Delta \tau \right);$$

$$\tilde{\Omega}^{(4)} = \frac{\Omega_0 \, \Omega_1^*}{2\Lambda} x;$$

$$S_k^{(4)} = \frac{|\Omega_k|^2}{4\Lambda} x.$$

Where $x=rac{|\Omega_0|^2+|\Omega_1|^2}{4\Delta^2}$ is the small parameter. After choosing $\tau>2\pi/\Delta$, $\beta(\tau)\to 1$.

References

- 1. Dowling, J.P.; Milburn, G.J. Quantum technology: the second quantum revolution. *Philosophical Transactions of the Royal Society of London. Series A: Mathematical, Physical and Engineering Sciences* **2003**, 361, 1655–1674.
- 2. Deutsch, I.H. Harnessing the power of the second quantum revolution. PRX Quantum 2020, 1, 020101.
- 3. Koch, C.P.; Boscain, U.; Calarco, T.; Dirr, G.; Filipp, S.; Glaser, S.J.; Kosloff, R.; Montangero, S.; Schulte-Herbrüggen, T.; Sugny, D.; et al. Quantum Optimal Control in Quantum Technologies. Strategic Report on Current Status, Visions and Goals for Research in Europe. 9, 19. https://doi.org/10.1140/epjqt/s40507-022-00138-x.
- 4. Nielsen, M.A.; Chuang, I. Quantum computation and quantum information, 2002.
- 5. Gisin, N.; Thew, R. Quantum communication. *Nature photonics* **2007**, *1*, 165–171.
- 6. Benenti, G.; D'Arrigo, A.; Falci, G. Enhancement of Transmission Rates in Quantum Memory Channels with Damping. *Phys. Rev. Lett.* **2009**, *103*, 020502. https://doi.org/10.1103/PhysRevLett.103.020502.
- 7. Degen, C.L.; Reinhard, F.; Cappellaro, P. Quantum sensing. Reviews of modern physics 2017, 89, 035002.
- 8. Bongs, K.; Holynski, M.; Vovrosh, J.; Bouyer, P.; Condon, G.; Rasel, E.; Schubert, C.; Schleich, W.P.; Roura, A. Taking atom interferometric quantum sensors from the laboratory to real-world applications. *Nature Reviews Physics* **2019**, *1*, 731–739.
- 9. Goerz, M.H.; Reich, D.M.; Koch, C.P. Optimal Control Theory for a Unitary Operation under Dissipative Evolution. *16*, 055012. https://doi.org/10.1088/1367-2630/16/5/055012.
- 10. Brown, J.; Sgroi, P.; Giannelli, L.; Paraoanu, G.S.; Paladino, E.; Falci, G.; Paternostro, M.; Ferraro, A. Reinforcement learning-enhanced protocols for coherent population-transfer in three-level quantum systems. *New Journal of Physics* **2021**, 23, 093035.
- 11. Giannelli, L.; Sgroi, P.; Brown, J.; Paraoanu, G.S.; Paternostro, M.; Paladino, E.; Falci, G. A tutorial on optimal control and reinforcement learning methods for quantum technologies. *Physics Letters A* **2022**, p. 128054.
- 12. Brion, E.; Pedersen, L.H.; Mølmer, K. Adiabatic elimination in a lambda system. *Journal of Physics A: Mathematical and Theoretical* **2007**, 40, 1033–1043.
- 13. Paulisch, V.; Rui, H.; Ng, H.K.; Englert, B.G. Beyond adiabatic elimination: A hierarchy of approximations for multi-photon processes. *The European Physical Journal Plus* **2014**, 129, 12.
- 14. Bravyi, S.; DiVincenzo, D.P.; Loss, D. Schrieffer–Wolff transformation for quantum many-body systems. *Annals of physics* **2011**, 326, 2793–2826.
- 15. Bukov, M.; Kolodrubetz, M.; Polkovnikov, A. Schrieffer-Wolff transformation for periodically driven systems: Strongly correlated systems with artificial gauge fields. *Physical review letters* **2016**, *116*, 125301.
- 16. Blanes, S.; Casas, F.; Oteo, J.; Ros, J. A pedagogical approach to the Magnus expansion. European Journal of Physics 2010, 31, 907.
- 17. Blanes, S.; Casas, F.; Oteo, J.; Ros, J. The Magnus expansion and some of its applications. *Physics Reports* **2009**, 470, 151–238.
- 18. Petiziol, F.; Arimondo, E.; Giannelli, L.; Mintert, F.; Wimberger, S. Optimized Three-Level Quantum Transfers Based on Frequency-Modulated Optical Excitations. 10, 2185. https://doi.org/10.1038/s41598-020-59046-8.
- 19. Vandersypen, L.M.; Chuang, I.L. NMR techniques for quantum control and computation. Reviews of modern physics 2005, 76, 1037.
- 20. Zhao, Q.; Zhou, Y.; Shaw, A.F.; Li, T.; Childs, A.M. Hamiltonian simulation with random inputs. arXiv preprint arXiv:2111.04773 2021.
- 21. An, D.; Fang, D.; Lin, L. Time-dependent unbounded Hamiltonian simulation with vector norm scaling. Quantum 2021, 5, 459.
- 22. Rajput, A.; Roggero, A.; Wiebe, N. Hybridized methods for quantum simulation in the interaction picture. Quantum 2022, 6, 780.
- 23. Haah, J.; Hastings, M.B.; Kothari, R.; Low, G.H. Quantum algorithm for simulating real time evolution of lattice Hamiltonians. *SIAM Journal on Computing* **2021**, pp. FOCS18–250.
- 24. Tran, M.C.; Guo, A.Y.; Su, Y.; Garrison, J.R.; Eldredge, Z.; Foss-Feig, M.; Childs, A.M.; Gorshkov, A.V. Locality and digital quantum simulation of power-law interactions. *Physical Review X* **2019**, *9*, 031006.
- 25. Berry, D.W.; Childs, A.M.; Su, Y.; Wang, X.; Wiebe, N. Time-dependent Hamiltonian simulation with L1-norm scaling. *Quantum* **2020**, 4, 254.
- 26. Vitanov, N.; Fleischhauer, M.; Shore, B.; Bergmann, K. Coherent manipulation of atoms and molecules by sequential laser pulses. *Adv. in At. Mol. and Opt. Phys.* **2001**, *46*, 55–190. https://doi.org/DOI:10.1016/S1049-250X(01)80063-X.
- Falci, G.; Di Stefano, P.; Ridolfo, A.; D'Arrigo, A.; Paraoanu, G.; Paladino, E. Advances in quantum control of three-level superconducting circuit architectures. Fort. Phys. 2017, 65, 1600077. https://doi.org/10.1002/prop.201600077.

- Vitanov, N.V.; Rangelov, A.A.; Shore, B.W.; Bergmann, K. Stimulated Raman adiabatic passage in physics, chemistry, and beyond. Rev. Mod. Phys. 2017, 89, 015006. https://doi.org/10.1103/RevModPhys.89.015006.
- 29. Siewert, J.; Brandes, T.; Falci, G. Advanced control with a Cooper-pair box: Stimulated Raman adiabatic passage and Fock-state generation in a nanomechanical resonator. *Phys. Rev. B* **2009**, *79*, 024504. 27 citazioni da citare per h index totale, https://doi.org/10.1103/PhysRevB.79.024504.
- 30. Falci, G.; Ridolfo, A.; Di Stefano, P.; Paladino, E. Ultrastrong coupling probed by Coherent Population Transfer. *Sci. Rep.* **2019**, *9*, 9249. arXiv 1708.00906, https://doi.org/10.1038/s41598-019-45187-y.
- 31. Di Stefano, P.G.; Paladino, E.; D'Arrigo, A.; Falci, G. Population transfer in a Lambda system induced by detunings. *Phys. Rev. B* **2015**, 91, 224506. https://doi.org/10.1103/PhysRevB.91.224506.
- 32. Vepsäläinen, A.; Danilin, S.; Paladino, E.; Falci, G.; Paraoanu, G.S. Quantum Control in Qutrit Systems Using Hybrid Rabi-STIRAP Pulses. *Photonics* **2016**, *3*, 62. https://doi.org/10.3390/photonics3040062.
- 33. Earnest, N.; Chakram, S.; Lu, Y.; Irons, N.; Naik, R.K.; Leung, N.; Ocola, L.; Czaplewski, D.A.; Baker, B.; Lawrence, J.; et al. Realization of a Lambda System with Metastable States of a Capacitively Shunted Fluxonium. *Phys. Rev. Lett.* **2018**, 120, 150504. https://doi.org/10.1103/PhysRevLett.120.150504.
- 34. Hays, M.; Fatemi, V.; Bouman, D.; Cerrillo, J.; Diamond, S.; Serniak, K.; Connolly, T.; Krogstrup, P.; Nygård, J.; Levy Yeyati, A.; et al. Coherent manipulation of an Andreev spin qubit. *Science* **2021**, *373*, 430–433.
- 35. Pellegrino, F.; Falci, G.; Paladino, E. 1/f critical current noise in short ballistic graphene Josephson junctions. Commun Phys 2020, 3, 6.
- 36. Di Stefano, P.; Paladino, E.; Pope, T.; Falci, G. Coherent manipulation of noise-protected superconducting artificial atoms in the Lambda scheme. *Physical Review A* **2016**, *93*, 051801.
- 37. Casas, F. Sufficient conditions for the convergence of the Magnus expansion. *Journal of Physics A: Mathematical and Theoretical* **2007**, 40, 15001.
- 38. Brinkmann, A. Introduction to average Hamiltonian theory. I. Basics. Concepts in Magnetic Resonance Part A 2016, 45, e21414.